Conversion-free Interleaved Black blood and Bright blood Imaging (cfIBBI) sequence for Dynamic Contrast Enhanced (DCE) MRI of vessel wall

Tingting Wu[1], Huijun Chen[1], Jinnan Wang[2], Juan Wei[3], Feiyu Li[4], and Chun Yuan[1,5]

[1]*CBIR, School of Medicine, Tsinghua University, Beijing, China,* [2]*Clinical Sites Research Program, Philips Research North America, Briarcliff Manor, NY, United States,* [3]*Philips Research Asia, Shanghai, China,* [4]*Peking University First Hospital, Beijing, China,* [5]*Dept. of Radiology, University of Washington, Seattle, WA, United States*

Introduction

Black-blood Dynamic Contrast-Enhanced (DCE) MRI of vessel wall has been used to detect early atherosclerosis[1] and monitor plaque progression[2]. Unlike traditional bright-blood techniques, thin vessel walls with early lesions can be clearly delineated without interference from lumen signal in black-blood DCE MRI. However, most existing black-blood DCE-MRI techniques for early diseased vessel walls use a simplified area under the curve (AUC) analysis[1], as the difficulty to extract arterial input function (AIF) from the black-blood DCE MRI precludes the kinetic analysis. To accurately estimate kinetic parameters for early atherosclerotic lesions, a sequence of interleaved black-blood and bright blood acquisition with high spatial and temporal resolution is needed. Recently, several sequences have been proposed, including IBBI[3], BB-SHILO[4], and SRDIR[5]. However, the signals from black-blood and bright-blood images are not comparable and require complex conversion for kinetic analysis in IBBI and BB-SHILO. In SRDIR, the blood suppression is not ideal for DCE acquisition and its temporal resolution is low. In this study, we propose a conversion-free interleaved black blood and bright blood sequence (cfIBBI), with excellent blood suppression and high spatial resolution in black blood images as well as high temporal resolution in bright blood images for AIF.

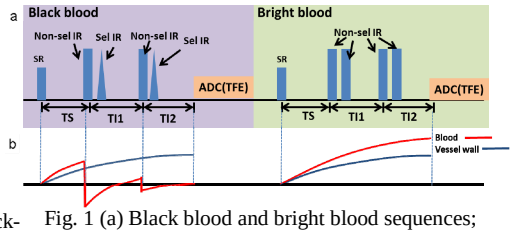

Fig. 1 (a) Black blood and bright blood sequences; (b) Signal of vessel wall and blood.

Methods

Black Blood Imaging: To create a T1-weighted black blood image, we used a TFE based sequence with a pre-pulse combining a non-selective Saturation-Recovery (SR) and Quadruple Inversion-Recovery[6] (QIR), as shown in the left figure of Fig. 1a. The SR pulse can generate T1 weighting and avoid interference between black-blood and bright-blood segments. The QIR pre-pulse is used to suppress the blood in a wide range of T1[6]. Blood flow into the imaging plane will experience one SR pulse and two IR pulses, while the tissue in the imaging plane will experience one SR pulse and four IR pulses. As a result, by optimizing the parameters of TS/TI1/TI2 (Fig. 1) according to:

$$[TS, TI1, TI2]\arg = \min \int_{T1_{\min}}^{T1_{\max}} \left| M_z^{blood}(TS, TI1, TI2, T1) \right| dT1$$

(M_z^{blood} is the longitudinal magnetization of blood, and $T1_{\max}$ and $T1_{\min}$ are the maximal and minimal T1 of blood during dynamic imaging, $T1_{\min}$ =200ms, $T1_{\max}$ = 1500ms, respectively), the signal of blood can be suppressed in a wide range of T1, with tissue recovery according to the T1 value.

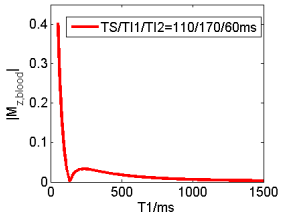

Fig. 2 Absolute value of longitudinal magnetization as function of T1 after optimization.

Bright Blood Imaging: To obtain comparable bright blood images, the bright blood sequence, especially its timing, is designed identically to the black blood acquisition, except that we replace the slice-selective pulses of QIR with non-selective pulses to generate T1-weighted blood signal (right figure of Fig. 1a).

Interleaved Timing Diagram: To obtain black-blood and bright-blood images simultaneously, segmented acquisition (black-blood segment and bright blood segment were interleaved) was used (Fig.3). To achieve high spatial and temporal resolution for kinetic analysis, we used different resolutions in black-blood and bright-blood acquisitions. Because vessel walls with early lesions are very thin and their signal changes slowly, they should be imaged with high spatial resolution. On the other hand, the lumen signal (AIF) changes rapidly, demanding higher temporal resolution. Hence, spatial resolution for black-blood acquisition was designed 4 times higher than bright blood images, and the temporal resolution for bright blood imaging was 4 times higher than black blood imaging.

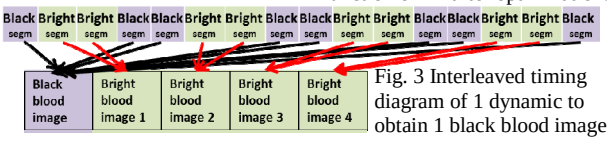

Fig. 3 Interleaved timing diagram of 1 dynamic to obtain 1 black blood image and 4 bright blood images.

MR Imaging: After institutional review board approval, a healthy New Zealand rabbit (3kg) was scanned on a 3.0T MR system (Achieva, TX, Philips) using a 8-channel knee coil. 0.1 mmol/kg of contrast (Gd-DTPA) was injected coincident with the third acquisition (black-blood dynamic) at a rate of 2ml/s following with 15ml saline solution. The scan parameters: TR/TE 7.5/3.7ms, flip angle 30°, TFE factor 20, TS/TI1/TI2= 110/170/60ms, FOV 80×80mm, slice thickness 6mm, 1 slice. Black blood images have a spatial resolution of 0.5×0.5mm, 15 dynamic scans, and temporal resolution 7.87s; while bright blood images have a spatial resolution of 0.5×2mm, 60 dynamic scans, and temporal resolution 1.97s.

Image analysis: Images were analyzed using a custom program written in Matlab (Mathworks Inc.). First, contours were manually drawn on each frame of the black-blood dynamic acquisition to segment the vessel wall. Then, by assuming a linear relationship between the MRI signal and contrast concentration, the normalized average intensity curve ((SI(t)-SI(0))/ SI(0), where SI(t) is the intensity at time t) of the vessel wall in black-blood images (Ct) was extracted as the contrast concentration curve for kinetic analysis. As black blood and bright blood images are acquired at different resolutions, zero-padding is used to expand the bright-blood matrix size to 160×160 before Fourier transform, so signals from black blood and bright blood images are comparable. Similarly to Ct, the AIF (Cp) was calculated from the lumen in bright-blood images. The Patlak model[7] was then used to calculate transfer constant (K^{trans}) and partial plasma volume (v_p) of the artery. The intensity of a muscle region is also reported to test the signal consistency between black-blood and bright-blood acquisition.

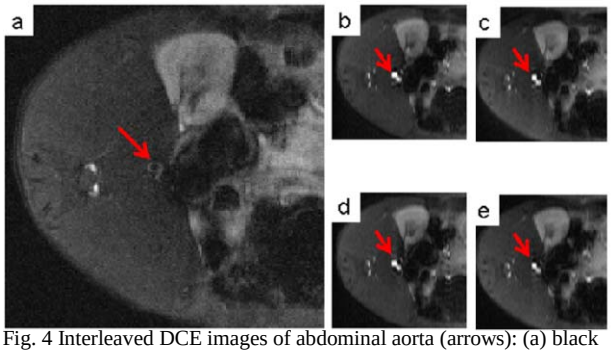

Fig. 4 Interleaved DCE images of abdominal aorta (arrows): (a) black blood image, post contrast, dyn=5, t=31.5s; (b)~(e) corresponding bright blood images, dyn=17,18,19,20, t=31.5s,33.5s,35.4s,37.4s.

Results

Fig.4 shows example images. Blood suppression is excellent after contrast arrival, and the vessel wall can be clearly seen in the black-blood images with high spatial resolution. At the same time, the bright-blood image is distinct, with a high temporal resolution of 1.97s. The Ct and AIF curves of the rabbit aorta are shown in Fig.5. Calculated K^{trans} and v_p are 0.074 min^{-1} and 0.165, respectively, reasonable in a normal artery by compared to values reported in previous study[2]. Also, average muscle signals in the black blood and the bright blood images are nearly the same, as shown in Fig.6.

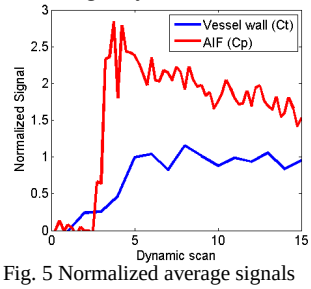

Fig. 5 Normalized average signals of vessel wall and AIF.

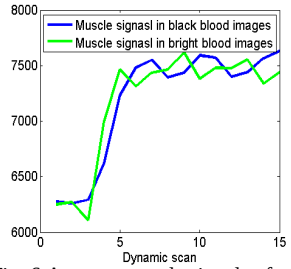

Fig. 6 Average muscle signals of muscle in black- and bright-blood images. (Muscle signals in every 4 bright blood images are averaged to match with black-blood images.)

Conclusion

In this study, a conversion-free Interleaved Black blood and Bright blood DCE-MR Imaging (cfIBBI) technique was developed to evaluate vessel wall perfusion of early lesion with excellent blood suppression. It offers simultaneous high spatial-resolution black blood acquisition to better image thin vessel walls and high temporal-resolution bright blood acquisition to catch the rapidly changing signals of AIF for kinetic analysis. Moreover, the intensities obtained from the black-blood and bright-blood images are comparable and can be directly used in kinetic analysis without conversion.

Reference: 1.C Calcagno et al. ATVB 2008, 1311-7. 2.H Chen et al. MRM 2012, 24415. 3.J. Wang et al. ISMRM 2011,1234. 4.P M Robson et al. ISMRM 2012, 321. 5. Z. Fan et al. ISMRM 2012, 3822. 6. Vasily L. et al. MRM 2002, 899-905. 7.CS Patlak. et al. JCBFM 1983, 215-225.